A fluid collection system for dermal wounds in clinical investigations

Michael Klopfer,[1] Derek Banyard,[1,2] G.-P. Li,[1] Alan Widgerow,[1,2] and Mark Bachman[1,a)]
[1]*Department of Biomedical Engineering, Henry Samuelli School of Engineering, University of California at Irvine, Irvine, California 92697, USA*
[2]*Department of Plastic Surgery, Center for Tissue Engineering, School of Medicine, University of California at Irvine, Orange, California 92868, USA*

(Received 26 November 2015; accepted 22 February 2016; published online 22 March 2016)

In this work, we demonstrate the use of a thin, self adherent, and clinically durable patch device that can collect fluid from a wound site for analysis. This device is manufactured from laminated silicone layers using a novel all-silicone double-molding process. *In vitro* studies for flow and delivery were followed by a clinical demonstration for exudate collection efficiency from a clinically presented partial thickness burn. The demonstrated utility of this device lends itself for use as a research implement used to clinically sample wound exudate for analysis. This device can serve as a platform for future integration of wearable technology into wound monitoring and care. The demonstrated fabrication method can be used for devices requiring thin membrane construction. © *2016 AIP Publishing LLC*.
[http://dx.doi.org/10.1063/1.4943133]

I. INTRODUCTION

Burn and chronic wound care and treatment is largely empirical, and continued studies are underway for improvement of current practices.[1,2] Exudate management and study of wound exudate including exudate cytokine content, chemical component analysis, and bacterial loads are important factors in establishing the effectiveness of treatments and improving patient outcome through interventional measures.[3–7] Up to now, the only ways to measure wound exudate were through manual aspiration using devices such as a syringe-needle combination or through the collection of fluid directly from the dressings after their removal from wounds.

It has recently been hypothesized that incremental observations of exudate cellular components and cytokine levels may greatly improve prognostic and therapeutic features of burn care treatment, in particular.[4] Currently, there are major issues in achieving incremental burn fluid collection in a practical and efficient manner. Manual aspiration, with a syringe-needle combination, for instance, requires repeated wound exposure with risk of further injury or infection. Alternatively, fluid collection from exudate-soaked dressings can prove extremely difficult: the cellular/protein attachment, as well as the fluid absorption and evaporation that occurs as exudate is drawn into the dressings not only modifies its concentration and distribution, but also results in unpredictable volumes that would preclude the incremental collection of exudate over an extended period of time. The case is the same for an alternative dressing approach using suction, negative pressure wound therapy (NPWT). This system can collect fluid as a byproduct of device operation, yet the volume and treatment area can be so large and the fluid collection delay so inconsistent that sampled aspirate has no direct temporal or spatial correlation to the wound site. To date, no device exists clinically to collect fluid from a large spatial area to permit temporal changes in exudate constituents.

a)Author to whom correspondence should be addressed. Electronic mail: mbachman@uci.edu. Tel.: +19498243732.

In general, dressing changes are typically painful and require skilled health-care worker time. Additionally, continual removal of dressings for analysis becomes practically difficult and exposes the patient to an increased infection risk. Alternatively, conventional surgical drains can be modified for use under dressings with some limited collection effectiveness. This off-label use is not taken into consideration in the engineering of these products and they perform poorly in this task and are prone to air leaks and blocked flow.

In this work, we designed a novel flat, self-adherent patch collection device that can be interfaced to a conventional aspiration collection system. This disposable device can be used to permit under-dressing extraction of fluid between dressing change periods. The internal volume of the collector is less than 250 μl. The total device collector thickness is 250 μm. Single layer thickness is 120 μm with an ultimate minimum thickness of 30 μm (between back to back features on both sides). Minimum feature size was 70 μm in width. Fluid channel width was 150 μm, depth was 90 μm. The design uses an external molded gasket system that reduces air intrusion between the skin and the device. The result is efficient fluid collection with minimal air intrusion. A 70 μm grid pitch of 90 μm tall columns were patterned on the patient interface side of the device to permit lateral fluid flow across the front of the device. Fluid is collected into the device through fluid vias and into a channel system internal to the device. Eventual fluid flow is to an interface connector and to a silicone tube that leads the fluid to an aspiration collection system.

The device was pre-clinically tested to verify even, consistent fluid collection. A limited clinical demonstration was performed with patient informed consent demonstrating the ability of this device to collect fluid from a wound site in a clinical environment from a partial thickness burn. Qualitative feedback was collected from this pilot study. The patient noted that this device produced no discomfort and was unobtrusive in use. Continued development of this technology can provide a clinical tool for use in assessing wound healing by providing a practical means for exudate collection for analysis.

II. MATERIALS AND METHODS

A. Design requirements and specifications

Clinical input was received in device design and construction. This device is intended to be used under dressings and must be thin, flat, and flexible. The device must be large enough to cover a clinically significant wound. A size of 4 $\times$ 4 cm square was chosen due ease of practical manufacture and practical size for extremity burns. The device must have limited internal dead space and provide even fluid collection across the surface in contact with the skin. A micro textured surface layer (using a grid pattern) was chosen to provide lateral flow to device inlets. The device must seal itself against the skin to prevent air from leaking into the collection system. A gasket micro feature was added for this purpose. The collection system must be passive. A system diagram for the collection device is shown in Figure 1.

A vacuum space is filled with collected fluid to provide fluid flow. No pumps are to be used. Air leaking in this situation would additionally reduce the strength of the vacuum during collection. The construction material must match the predicate design device (Stryker TLS Surgical Drainage System, Stryker Healthcare, Kalamazoo, MI, USA). We chose a platinum cured silicone polydimethylsiloxane (PDMS) elastomer (Dow Corning 184, Dow Corning, Midland, MI, USA) with well characterized material, fabrication, sterilization, and short-term biocompatibility properties.[8–15] The entire body of the device is constructed from this material. No additional solvents, agents, or treatment chemicals were used in construction. The outlet tubing is a commercially available platinum cured silicone (REF 60-;011-03, Helix Mark, Helix Medical, Carpinteria, CA, USA). Prior material tests proved strong, liquid-tight, and durable bonding between this tubing and PDMS elastomer cured onto it when the surface is treated with corona discharge. The tubing interface uses an irrigation syringe needle slipped onto the tube to provide a Luer-Lok interface connection. To provide the aspiration, a 30 ml VacLok locking vacuum syringe (VacLok 130, Merit Medical, South Jordan, UT, USA) is connected via the Luer-Lok connector.

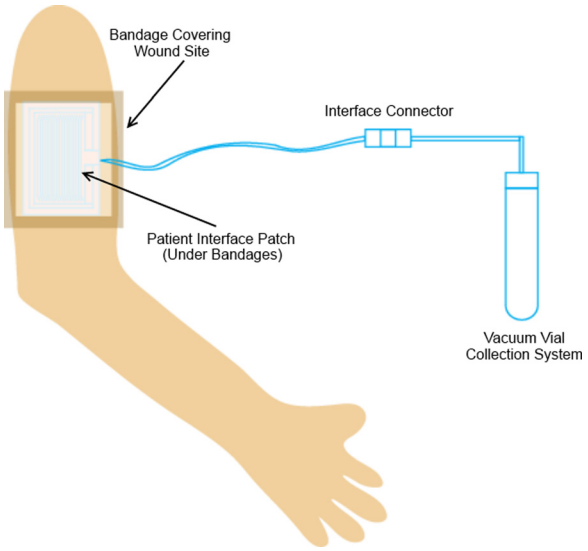

FIG. 1. Diagram of the constructed fluid collection system showing under dressing patch, silicone tubing, and example vacuum collection system.

B. Design and fabrication

The final device comprises three components: a membrane with features on both sides, a featureless membrane, and an interface connector. All device components are laminated together using aerosolized uncured PDMS as a layer adhesive. Layer bonding with oxygen plasma treatment is effective for assembly, and was evaluated by the authors, but was not used in clinical devices due to repeated edge delamination defects in completed devices.

1. Double-side feature membrane

Mold structures (in positive form) were individually milled onto polymethmethacrylate (PMMA) sheets using a CNC mill. Post CNC manufacture, both mold halves were washed in isopropanol, ultrasonic cleaned in distilled water, then rinsed in distilled water, and dried with nitrogen. The two PMMA molds were used for silicone casting.

Top and bottom PMMA molds were used to cast the PDMS elastomer. Dow Sylgard 184 was of new stock and mixed in a ratio of 10:1 as directed and degassed in centrifuge followed by vacuum. PDMS was cast on PMMA molds with a thickness of 5 mm to produce inter-molds. The cast PDMS was easily detached from the PMMA molds. PMMA molds are long-term reusable and placed in storage.

The fresh cast PDMS inter-molds are negatives of the final device structure. These PDMS inter-molds are used in a "waffle-iron" fashion to cast both sides of the final double sided PDMS membrane. A thin layer of uncured PDMS is cast between two anti-adhesive treated PDMS-inter-molds was used to produce the final double-sided membrane. As curing PDMS sticks to clean, cured PDMS readily, a significant problem exists. The two sides on the mold readily bond together and do not separate from the casted thin-membrane between them. Even if separation can occur for the mold halves, the thin membrane must be separated from both mold halves without ripping or damage to fine features. This is not a trivial problem, and proper separation requires a combination of the inter-mold anti adhesive coating and a spacer frame support for the casted membrane. A number of protocols typically involving polysiloxane or alkoxylsilane surface coating exist to prevent PDMS to PDMS adhesion and act as a mold release for casting.[16–20] A diagram of this fabrication process is shown in Figure 2.

Due to the clinical nature of this device, these additive requiring common protocols for en-vitro device construction would contaminate the final device with potentially toxic and medically uncommon substances and must be avoided for safety with en vivo human use.[21] As an

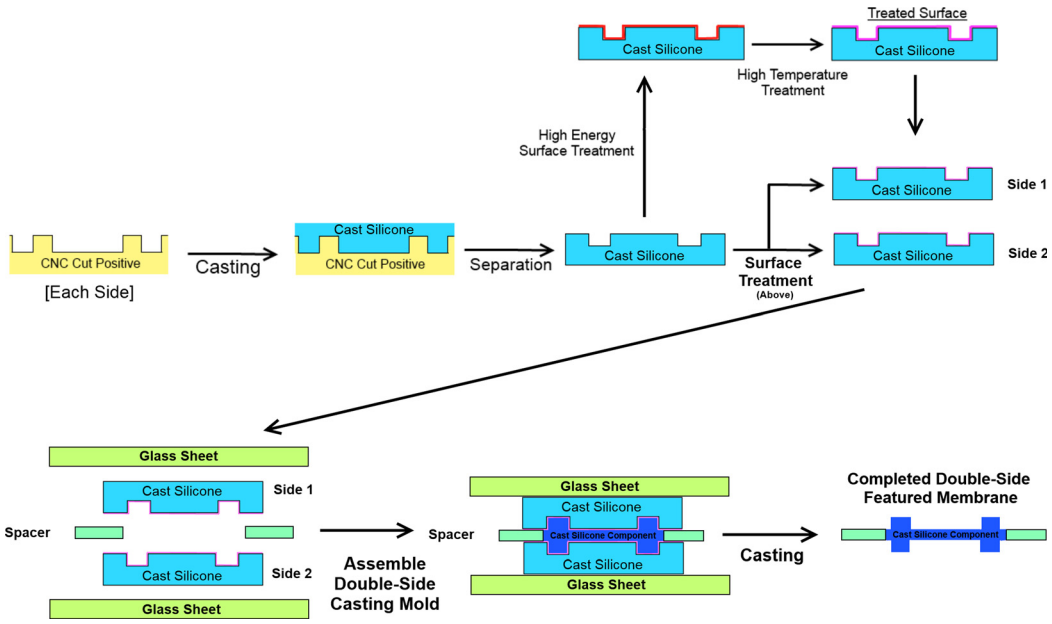

FIG. 2. Process diagram for the molding of a double side featured membrane.

alternative, we extended upon previous work to develop a non-additive based surface treatment for rapid thin membrane fabrication.[22–31] This process requires two steps—high energy surface treatment followed by high temperature treatment of the inter-molds. A PDMS-PDMS non-stick treated surface is formed on the surface that was high energy surface treated followed by rapid exposure to high heat. Freshly cured PDMS inter-molds are immediately treated with high energy surface treatment. Two commonplace high-energy surface treatment methods have been shown equally effective. Corona discharge treatment was made by placing the PDMS to be treated on a grounded metallic surface. The surface of the PDMS to be treated was manually treated with a soft copper brush connected to a 5000 V, 40 kHz RF source (Micro Mini Mite Tesla Coil, Information Unlimited, Mont Vernon, NH, USA). Alternatively, intense UV exposure has been used with satisfactory results. We have experimentally determined that 40 min minimum of exposure of an intensity of 73 mW/cm^2 from a commercial UV adhesive cure UV light source (Model 7401, Locktite, Henkel Corporation) is sufficient to permit eventual mold separation. Following high energy surface treatment, the PDMS surface is very susceptible to permanent bonding to both cured and uncured PDMS.[32,33] A second step of high temperature treatment is necessary to complete the surface anti-adhesive process to form a non-stick treated surface for uncured PDMS.[22] High energy surface treated PDMS inter-molds are immediately placed into a glass dish on top of a stainless steel mesh support with a lose fitting glass lid and then placed in an oven held at 220 °C for 30 min. For times less than 20 min or temperatures less than 150 °C, poor membrane separation was observed. Greater times and temperatures lead to mold embrittlement and reduced mold lifetime. After high temperature treatment time has elapsed, the glass dish is removed from the oven and allowed to cool. This process is repeated for both PDMS inter-molds. Typical treatments would last for the lifetime of the mold. Practical inter-mold lifetime was approximately 5–7 moldings before mold feature damage began to occur.

To cast thin, uniformly spaced, double featured membranes, inter-molds must be held flat and parallel during the casting process. This is accomplished using glass sheets to temporarily back the PDMS inter-molds during membrane casting. Soda-lime glass sheets are cleaned using isopropanol, rinsed with deionized water, and dried with nitrogen. The glass is treated with corona discharge to permit a temporary bonding of the flat underside of the treated PDMS inter-molds. This provides a force strong enough to hold the PDMS inter-mold to the glass

during casting, yet weak enough to easily remove it during mold disassembly. The PDMS inter-molds are trimmed to remove any rough edges or surface deformations and carefully pressed onto the glass with gloved hands. The same procedure is duplicated for the other inter-mold. Common inter-mold interface marks are superimposed, and easy-to-read alignment marks are made with grease pencil on the glass plates to permit easy gross mold alignment with fine alignment performed via microscopic inspection. The clear glass and clear PDMS inter-molds permit mold alignment using a visual process. A laser cut (VL-200 Versalaser, Universal Laser Systems, Scottsdale, AZ, USA) paper spacer frame is inserted between the molds. Standard hard bond copy paper was used. The thickness of this paper spacer sets the majority membrane thickness. For this study, paper of 95 μm thickness was used. Final membrane thickness was 120 μm. Liquid uncured PDMS is poured on the paper spacer and one mold. The two inter-mold glass halves are quickly assembled to ensure full PDMS coverage and then both halves are separated. Both inter-mold halves are placed in a vacuum and then carefully re-assembled, registered, and placed into an oven at 70 °C for 1 h on a flat surface with a 100 g scale-weight on top of the mold to prevent separation. After curing the assembly is removed from the oven and allowed to cool. The layers of the mold are carefully disassembled with light force. Disassembly is aided with isopropanol to improve layer separation and protect the membrane from point stress leading to tares during demolding. Membrane is demolded by flexing inter-molds with gentle pulling force on the spacer frame.

2. Featureless membrane

The second layer of the device is a thin (120 μm), flat, featureless membrane. This membrane is formed between two layers of rigid polycarbonate sheets. A paper spacer frame is used to set membrane thickness and provide a handling frame for transport and manipulation. The approach used to produce this type of membrane is variant of the "fluopon" technology developed for bio assays.[34] PDMS elastomer is mixed and degassed as previously described. Polycarbonate sheets are cleaned using isopropanol followed by a deionized water rinse and drying with nitrogen. A non-registered variant of the double-featured molding process is used to create the featureless membrane. For final curing, in place of an oven, both polycarbonate sheets are carefully reassembled after degassing and placed into a hot press (shown in Figure 3) with 1 kg of force and held at 70 °C for 2 h.

3. Device interface connector

The device interface connector is designed so that an indeterminate length of tubing can be connected to the device. The end of a silicone tube is placed snugly through a hole in a PMMA

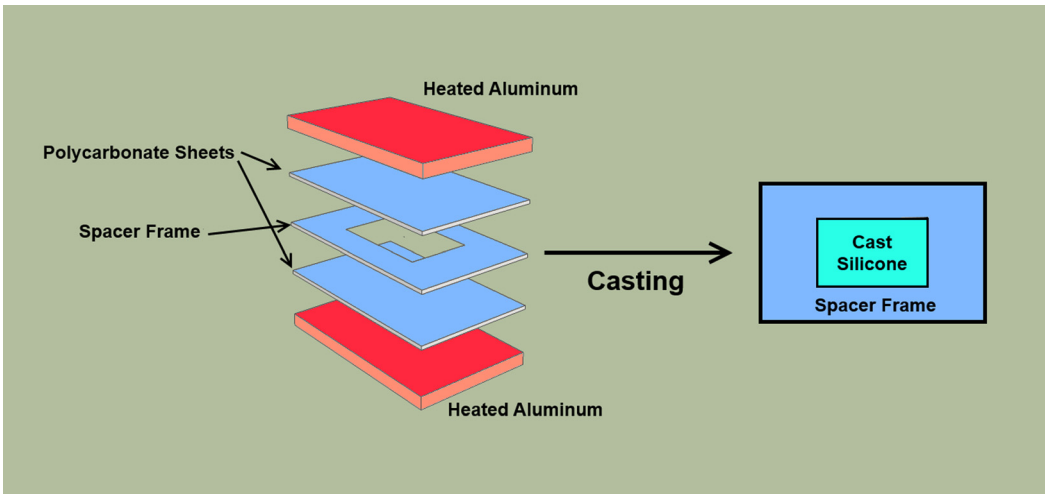

FIG. 3. Exploded diagram of the configuration used to cast flat, featureless membranes.

sheet just slightly larger than the tube itself. Premixed and degassed PDMS is carefully dropped on top of the tube at the PMMA interface from a beryl pipette to avoid air intrusion. The PMMA sheet and tube are placed in a curing oven at 70 °C for 1 h. After curing, a sharp shaving razor blade (Gillette Platinum Double Edge, Procter and Gamble, Boston, MA, USA) is passed along the surface of the PMMA to transect the tube and separate the PDMS from the PMMA.

C. Final device assembly

Device components are stored in a dust free environment before assembly. Both the flat membrane device is trimmed from the spacer frame using a razor. A 2 mm biopsy punch (BP-20F, Kai Medical, Solingen, Germany) is used to punch holes for collection and interface points. The membrane layers are placed on a flat surface, and a cosmetic airbrush (Master Performance G22, Master Airbrush, TCPGlobal, San Diego, CA) was used to apply a thin, atomized coat on the flat membrane side only. The authors find it important to note that a 10:1 hexane to uncured PDMS mixture applies easier when using an airbrush but was is not used in the manufacture of this device for patient safety reasons.[35] Device layers are carefully aligned and brought into contact. Assembly order is shown in an exploded diagram in Figure 4, and an assembly process diagram is shown in Figure 5. The completed device is cured in an oven at 70 °C for 1 h. Final device trimming is performed at this point.

The collection interface component is coated with uncured PDMS using a beryl pipette. The interface connector is mated to the interface hole punched into the featureless membrane and the device is cured in an oven at 70 °C for 1 h. An irrigation needle is fitted into the end of the outlet silicone tube to provide fluidic interfacing. Deionized water was flowed from a sterilized syringe into the device (reverse conventional flow) to verify flow integrity of the device and proper fluid flow. The final device (shown in Figures 6(a) and 6(b)) is treated in an ultrasonic cleaner, finish rinsed in deionized water, dried with nitrogen, and sealed in an air-tight chamber prior to autoclaving or use in flow performance testing. No flow performance tested devices were used clinically for cross-contamination reasons.

D. Flow performance testing

A test setup was created to simulate fluid flow from a wound and measure device collection performance. A PMMA sheet with 12 silicone tube inlets was created. A filter paper spacer (Whatman 1001, GE Life Sciences, Pittsburgh, PA, USA) was placed over this PMMA sheet and the device under test was placed on top. Adhesive tape was used to prevent air intrusion and force flow through the filter paper. All tubes were routed along a common path back to a common reservoir at a constant level with a single inlet-outlet port. This port was connected to a syringe pump set to provide constant fluid flow of deionized water at a rate of 1 ml/min.

The entire fluid system was purged of air and a dilute solution of 25 μm fluorescent green microspheres (Polybead YG, Polysciences, Warrington, PA, USA) was added to the fluid. A long wave UV light source (UVL-21, UVP, Upland, CA, USA) and high speed camera (EX-FH100, Casio Computer Co., Tokyo, Japan) were used to measure progression of individual beads. Capture rate was 60 frames per second. Frame-by-frame image analysis from video was performed in ImageJ (NIH, Bethesda, MD, USA). An experimental setup diagram is shown in Figure 7. The high fluorescence of the microspheres and internal camera UV filtration permits direct illumination of microspheres with focus set on the microsphere plane. In low concentration, individual microspheres are clearly visible as point light sources without additional magnification. A laser-cut scale below the tube of known diameter with 1 mm increments engraved is used to correlate bead velocity between multiple collection points. Ten bead velocities for each tube are averaged to report an approximated flow velocity. These average rates are compared inter-tube as a metric for flow performance.

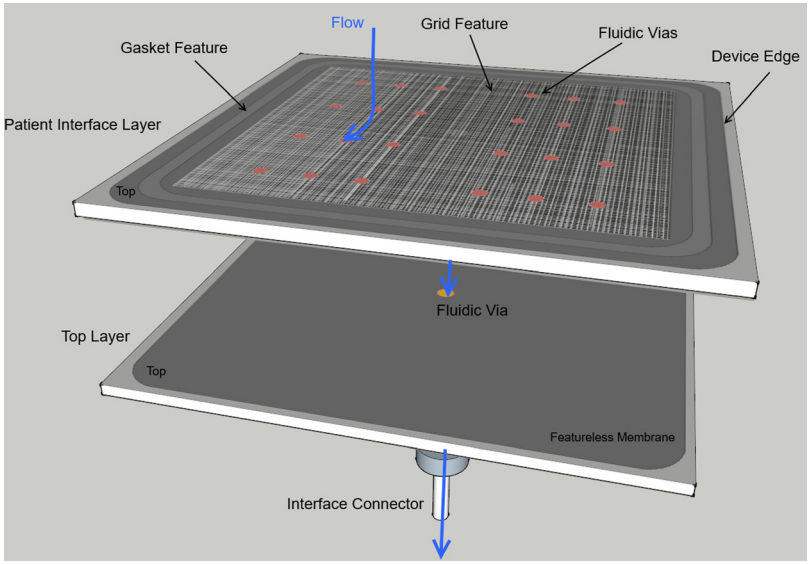

(a)

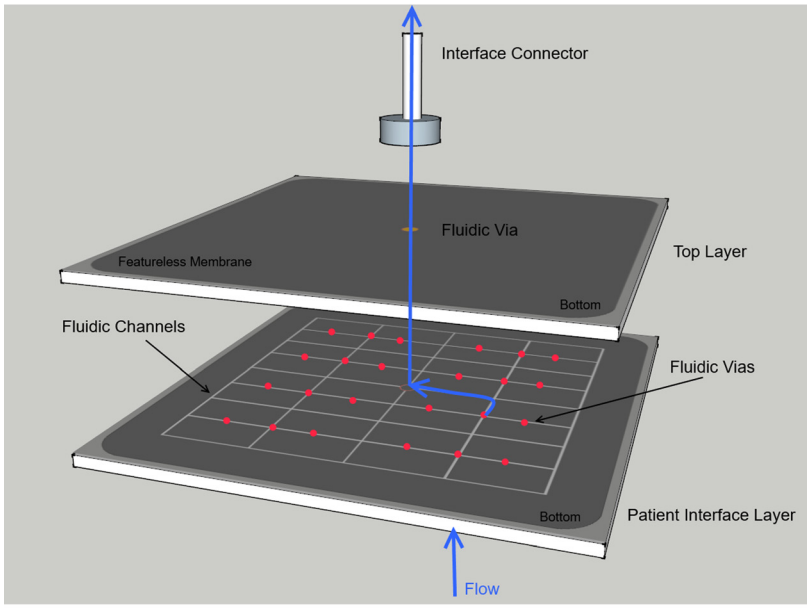

(b)

FIG. 4. An exploded 3D model of the device layers showing micro features, fluidic vias, and layer alignment. Two views are shown (top and bottom) with common outline alignment and trim lines. A hypothetical point source of liquid is shown to illustrate liquid flow in the device.

E. Clinical demonstration

Informed patient consent and institutional IRB approval (HS# 2013-9294) were obtained before clinical tests were performed. Devices were sterilized using a clinical autoclave protocol and handled using clinical protocols for transportation of surgical instruments post-sterilization. Within 24 h of patient presentation to the burn intensive care unit, a partial-thickness burn site was selected and the device was placed on the wound after it was cleaned per the burn admission protocol. A new sterile packaged vacuum syringe was connected to the outlet connector and a vacuum drawn after device priming with sterile saline. The patient was then questioned to the level of comfort associated with the device. Once adequate suction was established and maintained, an adherent surgical film was placed over the burn site to ensure skin sealing.

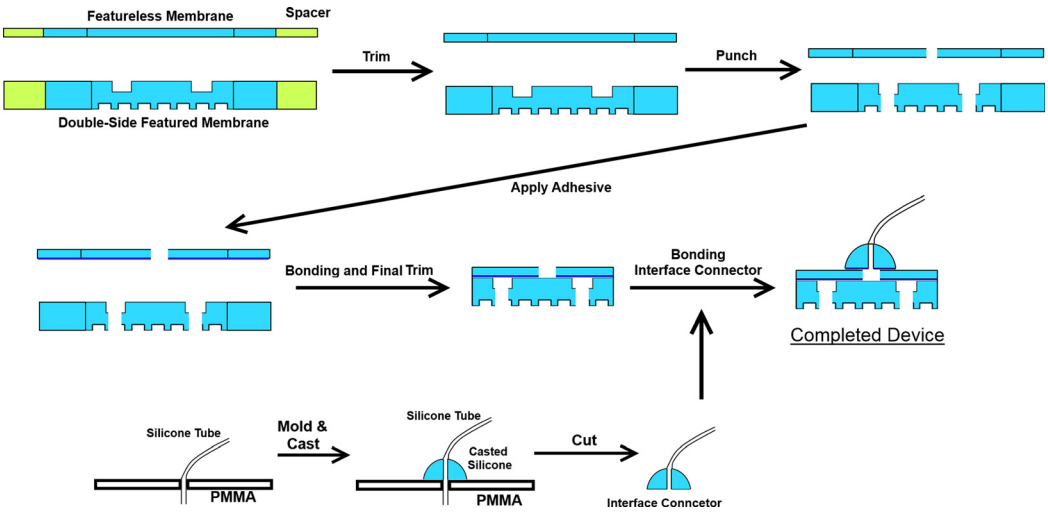

FIG. 5. Diagram of the assembly process used to laminate device components into final device.

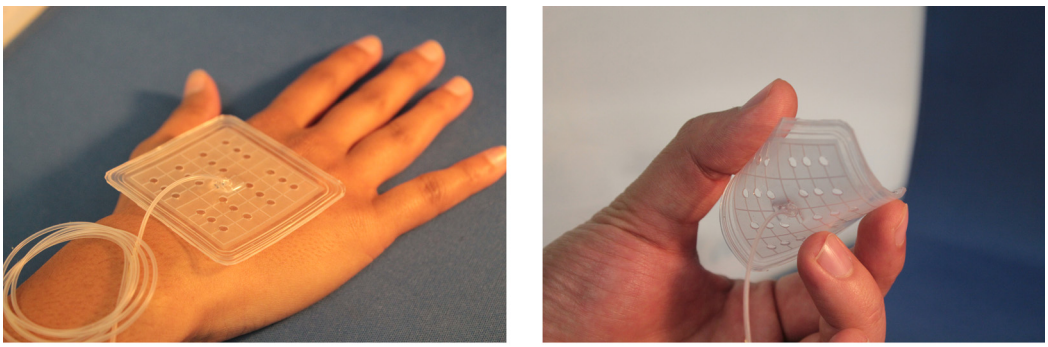

FIG. 6. Photographs of the final device showing size and flexibility.

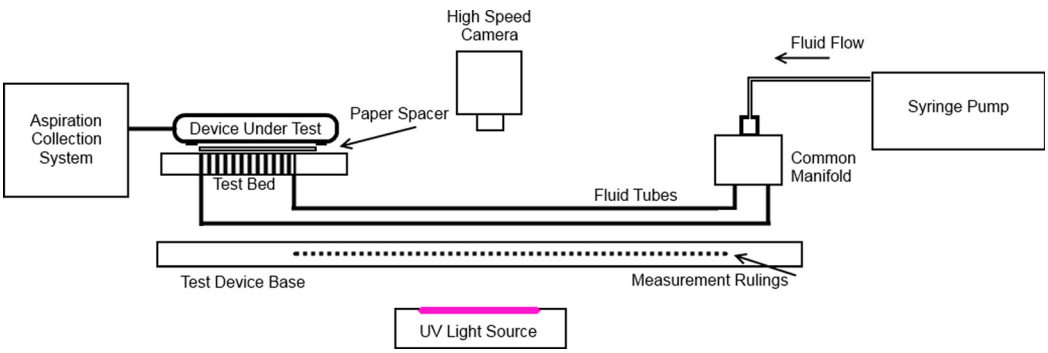

FIG. 7. Diagram of the flow performance testing setup showing the flow and imaging configuration.

Continued observations on device performance and the comfort of the patient were collected periodically by the nursing staff. At each time point, the collected fluid was deposited into sample vials for follow-up exudate component analysis and a new vacuum syringe was applied to the collection device.

III. RESULTS

A. Mechanical evaluation and flow performance testing

Sylgard 184 cured in the manner described in this experiment produces a hardness of 43 Shore A.[36] To test flexibility we evaluated the force to hold the device rolled across a 10 cm cylinder with one side anchored via a clip. A force gauge was driven with a micro positioner to apply a common force across the opposite side of the device to the anchored side. Micro positioner advancement was stopped and force measured when device-cylinder contact was made. This force was measured as 0.05 N and 0.041 N for the two devices tested.

Dynamic flow and collection profile were tested for two devices. When supplied flow was set to 1 ml/min, flow measurement of the tube with the highest mean velocity of the particles in

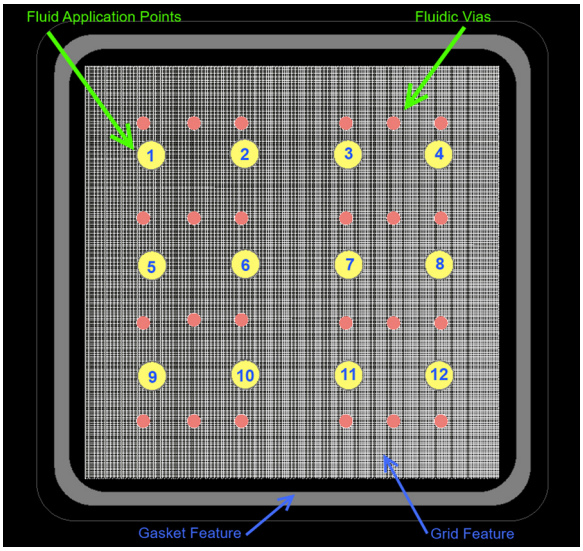

(a)

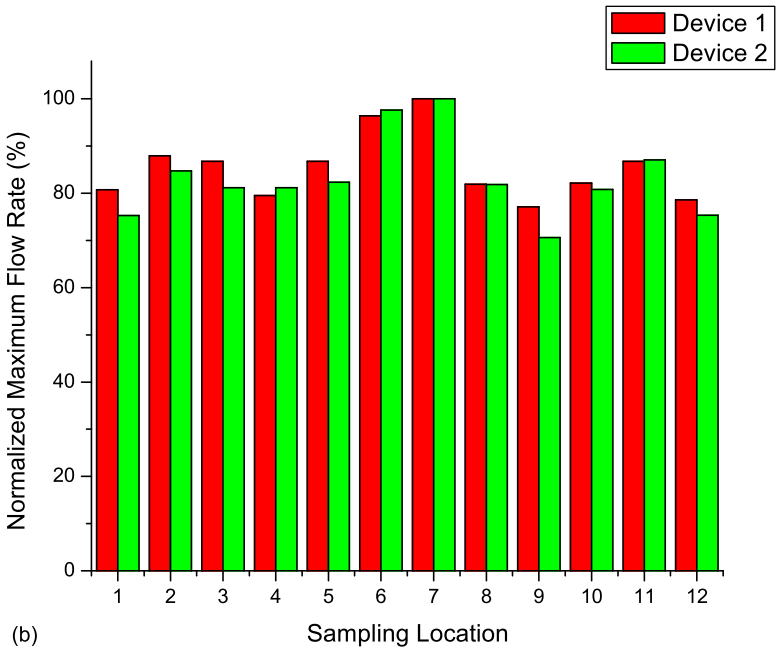

(b)

FIG. 8. (a) Diagram of the fluid sampling locations (yellow) along with the inter-layer vias (red). Fluid is emitted from the sampling locations, across the grid structure of the front of the device and into nearby fluidic vias during collection. (b) Corresponding sampling locations are compared for maximum observed flow rate and normalized across the global maximum flow rate.

flow was 0.502 cm/s and 0.514 cm/s, respectively, for the two devices tested. This is in accordance with estimated values. The diameter of the observation tube was 0.635 mm. Volumetric flow distributed across 12 tubes would correspond to a plug flow velocity of 0.44 cm/s. The physical location of the outlet tubes are shown in Figure 8(a). As laminar flow is assumed (with parabolic flow distribution), a distribution is expected and observed. A maximum difference in average flow rate across the device was shown to be 23% and 25%, respectively, for the two devices tested. The lowest observed mean velocities were on the corners of both devices at 0.387 cm/s (point 9 on device 1) and 0.386 cm/s (point 12 on device 2). Flows and flow patterns were remarkably consistent between the two devices tested, as shown in Figure 8(b).

B. Clinical demonstration

With informed consent, the device was tested at the UCI medical center on a patient presenting upper extremity partial thickness burns (Figure 9). Collection rate was approximately 5–6 ml in a sampling period of 5–6 h sampling time. The device was used for a period of 48 h and recharged between sampling periods. Leak rate was minimal, yet it was noted that a full vacuum charge was necessary to permit continued collection over a 5–6 h period. After this period residual vacuum likely begins to drop to the point where collection efficiency is substantially reduced. The area where the patch was applied was isolated with film dressing for the entire period. This was used as an additive measure to prevent air intrusion. Likely leaks can be reduced by more extensive application of sealing film dressing. The use of this device did not interfere with routine dressings or management of the patient. Pain was not reported by the patient. Clinical staff and the patient made the following practical observations and comments.

1. Less fluid was collected with this device than anticipated with the case presented. Device was very helpful for exudate sampling during fixed sampling periods, and likely the only practical approach for collecting sufficient exudate for analysis.
2. The use of a vacuum syringe was helpful and it made the collection and vacuum recharging process simple.
3. No pain was observed during suction, no observable irritation or swelling was present after device use and removal.
4. A long interface tube is necessary to permit placement of the vacuum syringe in a convenient location for long term sampling. In this case, the breast pocket was used as preferred by the patient.

IV. DISCUSSION

Fluid collection with even collection rates across a distributed area is a challenging problem. This challenge is exacerbated with requirement of a thin collection system. To permit

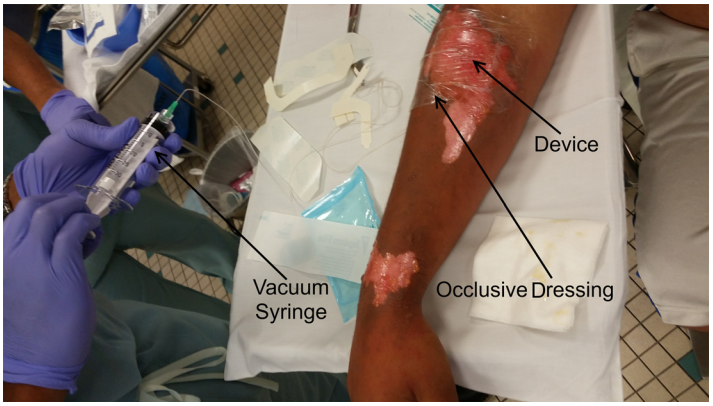

FIG. 9. Photograph of clinical demonstration showing device during collection under occlusive film dressing.

even collection, a device must produce an even pressure gradient (vacuum) across the collection area. Laminar fluid flow in a thin channel (modeled with a circular cross section) follows the Navier-Hagen-Poiseuille relationship where resistance to fluid flow is proportional to channel length (L) and fluid viscosity (μ) and inversely proportional to radius (r) to the 4th power. A constant of $\pi/8$ is commonly used to incorporate temperature and friction effects of smooth walled long cylindrical flow capillary. This value, commonly known as K″ can be calculated more precisely in further developed models.[37] Volumetric flow (Q) is proportional to pressure difference (ΔP) and inversely proportional to flow resistance (R)[37,38]

$$R = \frac{8 * L * \mu}{\pi * r^4},$$

$$Q = \frac{P_1 - P_2}{R} = \frac{\Delta P * \pi * r^4}{8 * L * \mu}.$$

For small rectangular channels, the channel cross-sectional dimensions (B and W) can be used to calculate volumetric flow similarly to a circular channel

$$Q = \frac{\Delta P * 2 * B^3 * W}{3 * L * \mu}.$$

The use of larger channels greatly increases flow for a given length channel. Yet with common tube sizing, length has the predominant effect with respect to resistance to fluid flow in a collection device. The practical effect observed is the inlets further away from a common manifold will have greater resistance to flow than closer inlets, creating a disproportional collection profile. For the designed device, if all resistance in the collection device is far less than the inherent "resistance" to fluid flow provided by the fluid emitting tissue, collection vacuum remains high and constant across the device. This does not inherently solve the disproportionate flow concern. To address this directly as well as changes in flow patterns by debris in practical usage, we designed an "indeterminate pathway" flow pattern. A grid pattern in the front of the device provides lateral flow channels. Capillary action wicks fluid into these channels to nearby fluidic vias. Within the internal portion of the device, interlinked channels provides redundant pathways for fluid to the central collection point. These two systems work hand in hand to distribute even vacuum across the collection area and evenly collect low volume fluid flow into the device in a consistent manner.

In development, forerunners of this reported device used individual pathways to the collection point. If debris or air bubbles block a pathway, this section of the device becomes deactivated, reducing collection from this area. In micro/meso scale fluidics, the surface tension of the air-liquid interface prevents easy clearing of bubbles in the device unless sufficient pressure is present to clear these obstructions. This forces the requirement that the device must be primed with saline prior to use. With multiple flow pathways, the fluid will follow the path of least resistance and blockage can remain. Air induction into the device can lead to pathway blockage. The device is self adherent due to device flexibility and a raised gasket on the patient interface section. This property is best demonstrated on moist smooth skin without debris or hair. A raised gasket feature on the patient interface side of the device provides sealing capability. To improve sealing, surgical film can be used to eliminate possible air sources. Rough skin or debris can prevent the self-adherence of the device.

Flow rate is proportional to pressure difference; the vacuum syringe in optimum conditions can produce an ultimate vacuum down to the vapor pressure of water at a given temperature.[39] Typically, air intrusion reduces the vacuum level. Estimation of this reduction can be made via the ideal gas law. In clinical use, when samples are to be collected, the locking syringe is unlocked, emptied, and recharged with vacuum. If vacuum suction is lost, restoration is easily accomplished by recharging the vacuum in the syringe. This use protocol worked well in a clinical setting and was unobtrusive to the patient or clinical staff. Continued research will use this

device for exudate collection for cytokine analysis. This initial study has created a device that works well in a clinical setting.

Collection of debris within the device, thereby hindering device performance, is always a concern. The built in redundancy of flow pathways within the device and the inherent filtering capability of the grid textured patient interface membrane provides some protection against debris, yet with this being said, the wound should be cleaned and cleared of major debris prior to device application.

Device lifetime is expected to be in the order of several days maximum as required by the intended use as a study device. The device is constructed from silicone elastomer which has historically been used in medical devices, and we expect no biocompatibility issues with short term use. Bacterial load and odor is always a concern as all burn wounds have a bacterial load. Replacement of a device is planned to be scheduled with each dressing change to prevent these issues for endangering patient safety. Alternate long term usage outside of the specified application would need to be carefully evaluated.

V. CONCLUSIONS

This work demonstrates a novel construction method for practical silicone for patient care applications. Benchmarking of the device showed a comparable fluid flow can be achieved across the device collection region. The device performed acceptably in a limited clinical demonstration. Future iterations of this device can serve as a patient care platform with integrated smart bandage technology to measure temperature, pH, oxygenation, and other wound care parameters to better evaluate the state of wounds. Further clinical study is necessary to assess device performance in collection of exudate on a variety of presented wounds.

ACKNOWLEDGMENTS

The authors would like to acknowledge and thank Liang (Lily) Wu and Jay Sheth for their assistance in developing the fabrication methods discussed in this publication.

This work was supported in part by the National Center for Research Resources and the National Center for Advancing Translational Sciences, National Institutes of Health, through Grant No. UL1 TR000153 and the CIRM training Grant Award No. TG2-012252 from the University of California, Irvine.

[1]D. N. Herndon, *Total Burn Care*, 4th ed. (Saunders Elsevier, 2012).
[2]A. Widgerow, Private Conversation (2013).
[3]A. D. Widgerow, "Chronic wound fluid—Thinking outside the box," Wound Repair Regener. **19**, 287–291 (2011).
[4]A. D. Widgerow, "The burn wound exudate—An under-utilized resource," Burns **41**, 11–17 (2015).
[5]I. Ono, H. Gunji, J. Zhang, K. Maruyama, and F. A. Kaneko, "Study of cytokines in burn blister fluid related to wound healing," Burns **21**, 352–355 (1995).
[6]E. Mikhal'chik *et al.*, "Comparative study of cytokine content in the plasma and wound exudate from children with severe burns," Bull. Exp. Biol. Med. **148**, 771–775 (2009).
[7]C. C. Finnerty, D. N. Herndon, D. L. Chinkes, and M. G. Jeschke, "Serum cytokine differences in severely burned children with and without sepsis," Shock **27**, 4–9 (2007).
[8]A. Mata, A. J. Fleischman, and S. Roy, "Characterization of polydimethylsiloxane (PDMS) properties for biomedical micro/nanosystems," Biomed. Microdevices **7**, 281–293 (2005).
[9]S. Halldorsson, E. Lucumi, R. Gómez-Sjöberg, and R. M. Fleming, "Advantages and challenges of microfluidic cell culture in polydimethylsiloxane devices," Biosens. Bioelectron. **63**, 218–231 (2015).
[10]J. Friend and L. Yeo, "Fabrication of microfluidic devices using polydimethylsiloxane," Biomicrofluidics **4**, 026502 (2010).
[11]Y. Xia and G. M. Whitesides, "Soft lithography," Annu. Rev. Mater. Sci. **28**, 153–184 (1998).
[12]J. R. Anderson, D. T. Chiu, H. Wu, O. J. Schueller, and G. M. Whitesides, "Fabrication of microfluidic systems in poly (dimethylsiloxane)," Electrophoresis **21**, 27–40 (2000).
[13]E. Ostuni, R. Kane, C. S. Chen, D. E. Ingber, and G. M. Whitesides, "Patterning mammalian cells using elastomeric membranes," Langmuir **16**, 7811–7819 (2000).
[14]M. Liu, J. Sun, Y. Sun, C. Bock, and Q. Chen, "Thickness-dependent mechanical properties of polydimethylsiloxane membranes," J. Micromech. Microeng. **19**, 035028 (2009).
[15]M. Zhang, J. Wu, L. Wang, K. Xiao, and W. A. Wen, "Simple method for fabricating multi-layer PDMS structures for 3D microfluidic chips," Lab Chip **10**, 1199–1203 (2010).
[16]J. Luo, E. Nelson, G.-P. Li, and M. Bachman, in *IEEE 63rd. Electronic Components and Technology Conference (ECTC)* (IEEE, 2013), pp. 1905–1911.

[17]J. Luo, E. L. Nelson, G. Li, and M. Bachman, "Microfluidic dielectrophoretic sorter using gel vertical electrodes," Biomicrofluidics **8**, 034105 (2014).
[18]G. To'a Salazar *et al*., "Micropallet arrays for the separation of single, adherent cells," Anal. Chem. **79**, 682–687 (2007).
[19]M. A. Shoffner, J. Cheng, G. E. Hvichia, L. J. Kricka, and P. Wilding, "Chip PCR. I. Surface passivation of microfabricated silicon-glass chips for PCR," Nucl. Acids Res. **24**, 375–379 (1996).
[20]K. Kim, S. W. Park, and S. S. Yang, "The optimization of PDMS-PMMA bonding process using silane primer," BioChip J. **4**, 148–154 (2010).
[21]P. A. Jean *et al*., "Chlorosilane acute inhalation toxicity and development of an LC50 prediction model," Inhalation Toxicol. **18**, 515–522 (2006).
[22]G. Shao, J. Wu, Z. Cai, and W. Wang, "Fabrication of elastomeric high-aspect-ratio microstructures using polydimethylsiloxane (PDMS) double casting technique," Sens. Actuators A: Phys. **178**, 230–236 (2012).
[23]J. R. Anderson *et al*., "Fabrication of topologically complex three-dimensional microfluidic systems in PDMS by rapid prototyping," Anal. Chem. **72**, 3158–3164 (2000).
[24]H. Wu, T. W. Odom, D. T. Chiu, and G. M. Whitesides, "Fabrication of complex three-dimensional microchannel systems in PDMS," J. Am. Chem. Soc. **125**, 554–559 (2003).
[25]Y. Luo and R. N. Zare, "Perforated membrane method for fabricating three-dimensional polydimethylsiloxane microfluidic devices," Lab Chip **8**, 1688–1694 (2008).
[26]J. C. Love, J. R. Anderson, and G. M. Whitesides, "Fabrication of three-dimensional microfluidic systems by soft lithography," MRS Bull. **26**, 523–528 (2001).
[27]D. Irimia and M. Toner, "Cell handling using microstructured membranes," Lab Chip **6**, 345–352 (2006).
[28]Y. Berdichevsky, J. Khandurina, A. Guttman, and Y.-H. Lo, "UV/ozone modification of poly (dimethylsiloxane) microfluidic channels," Sens. Actuators B: Chem. **97**, 402–408 (2004).
[29]M. Hagedon and J. A. Heikenfeld, "Hybrid of microreplication and mask-less photolithography for creating dual porosity and textured surface membranes," J. Micromech. Microeng. **23**, 117005 (2013).
[30]N. Lucas, S. Demming, A. Jordan, P. Sichler, and S. Büttgenbach, "An improved method for double-sided moulding of PDMS," J. Micromech. Microeng. **18**, 075037 (2008).
[31]P. K. Yuen and V. N. Goral, "Low-cost rapid prototyping of flexible microfluidic devices using a desktop digital craft cutter," Lab Chip **10**, 384–387 (2010).
[32]K. Haubert, T. Drier, and D. Beebe, "PDMS bonding by means of a portable, low-cost corona system," Lab Chip **6**, 1548–1549 (2006).
[33]M. A. Eddings, M. A. Johnson, and B. K. Gale, "Determining the optimal PDMS–PDMS bonding technique for microfluidic devices," J. Micromech. Microeng. **18**, 067001 (2008).
[34]S. Saedinia, K. L. Nastiuk, J. J. Krolewski, G. Li, and M. Bachman, "Laminated microfluidic system for small sample protein analysis," Biomicrofluidics **8**, 014107 (2014).
[35]J. H. Koschwanez, R. H. Carlson, and D. R. Meldrum, "Thin PDMS films using long spin times or tert-butyl alcohol as a solvent," PLoS One **4**, e4572 (2009).
[36]Dow Corning Sylgard 184 Silicone Elastomer Product Specification, Form 06-1009-01.
[37]S. R. Sutera, "The history of Poiseuille's law," Annu. Rev. Fluid Mech. **25**, 1–20 (1993).
[38]Fluid Flow Viscosity Poiseuille's Law, Visual Physics.
[39]W. M. Haynes, *CRC Handbook of Chemistry and Physics* (CRC press, 2013).